Trabajos de Geología, Universidad de Oviedo, 30 : 241-245 (2010)

Oviedo (Spain) 1-3 July 2008 International Meeting of Young Researchers in Structural Geology and Tectonics
ORSGET

Reliability of magnetic fabric as paleostress indicator: a case study in Miocene lacustrine sediments from the Ebro foreland basin, N Spain

R. SOTO[1*], J. C. LARRASOAÑA[1], L. E. ARLEGUI[2], E. BEAMUD[1], B. OLIVA[2,3] AND J. L. SIMÓN[2]

[1]*Lab. Paleomagnetismo, Instituto de Ciencias de la Tierra Jaume Almera, CSIC, Barcelona, Spain.*

[2]*Dpto. Ciencias de la Tierra, Universidad de Zaragoza, Pedro Cerbuna 12, 50009 Zaragoza, Spain.*

[3]*Now at: University of Karlsruhe, Hertzstrasse 16, 6.36. 76187 Karlsruhe, Germany.*

**e-mail: rsoto@ija.csic.es*

Abstract: This work deals with the comparison between ASM results from weakly deformed mudrocks that crop out at the internal part of the Ebro foreland basin and paleostress analyses obtained from fault populations and joint sets developed on limestone beds interbedded with the mudrocks. The coaxiality found between the magnetic and paleostress ellipsoids shows the validity of AMS studies as paleostress indicators in foreland basins when sampling is restricted to weakly deformed mudrocks.

Keywords: anisotropy of magnetic susceptibility, paleostress analysis, Ebro basin, weak deformation, mudrocks.

The anisotropy of magnetic susceptibility (AMS) is a fast and non-destructive technique that allows us to characterize even very subtle rock fabrics and provides valuable information on the formation and subsequent deformational history of rocks (Tarling and Hrouda, 1993). The study of magnetic fabrics can be used as paleostress indicators in weakly deformed sediments. However, there are few cases where the reliability of such magnetic fabrics has been contrasted with paleostress results (Kissel *et al.*, 1986; Mattei *et al.*, 1997; Borradaile and Hamilton, 2004).

In this work, we present ASM results from weakly deformed mudrocks that crop out at the central part of the Ebro foreland basin, in northern Spain (Fig. 1). These results are combined with previously published (Arlegui and Simón, 1998, 2001; Simón *et al.*, 1999) and new paleostress results obtained from fault populations and joint sets developed on limestone beds interbedded with the mudrocks. The goal of this work is to realize a systematic comparison of AMS and paleostress results on local and regional scales in order to examine the reliability of AMS data as a paleostress indicator.

Geological setting

The Ebro basin is a triangular-shaped basin that formed during the Tertiary at the foreland of the fold-and-thrust belts of the Pyrenees, the Iberian, and the Catalan Coastal Ranges (Alonso-Zarza *et al.*, 2002) (Fig. 1). It comprises a continuous sequence of Latest Eocene, Oligocene and Miocene continental sediments.

We have studied two sectors in the internal part of the basin characterised by different fracture systems in order to compare them with AMS results: the Monegros area (central part of the basin) and the Bardenas Reales area (northwestern part of the basin) (Fig. 1).

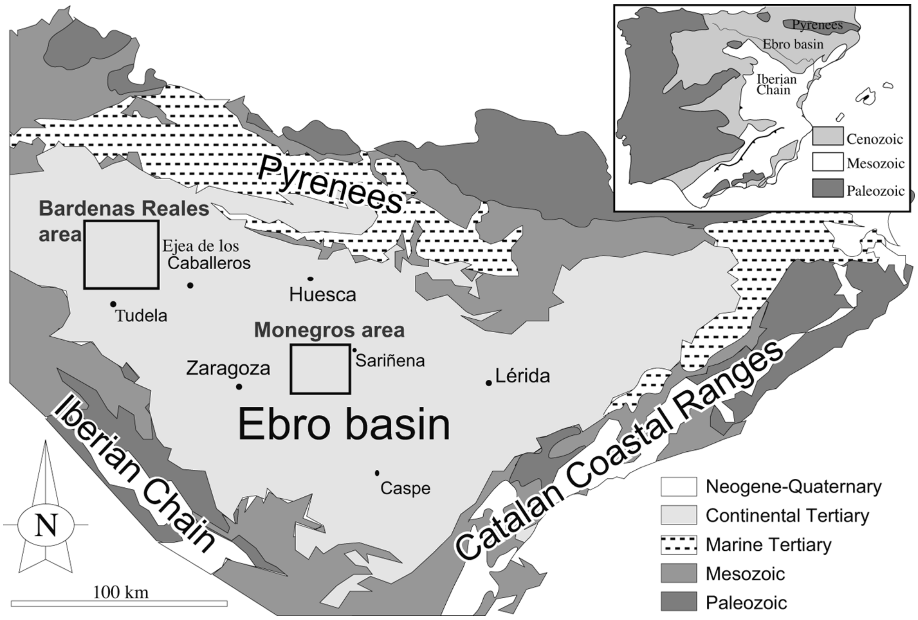

Figure 1. Geological sketch map of the Ebro basin, with location of the Bardenas Reales and Monegros areas shown in figures 2 and 3.

Brittle mesostructures in the internal sector of the Ebro basin

Continental sediments of the internal sector of the Ebro basin are affected by different fracture systems that include several joint sets as well as reverse, strike-slip and normal faults (Arlegui and Simón, 1998; 2001; Simón *et al*., 1999). The excellent exposure conditions allow determination of the geometry and timing relationships between different fracture systems, which developed according to the following general sequence: 1) E-W-trending reverse faults, 2) NNW- to NNE-trending strike-slip faults, 3) N-S-trending joints, 4) N- to NE-trending normal faults, and 5) E-W-trending joints. E-W-trending reverse faults are scarce and, together with NNW- to NNE-trending strike-slip faults, are only found at the Bardenas Reales area. N-S-trending joints are systematic and ubiquitous throughout the internal part of the Ebro basin. N- to NE-trending normal faults are also ubiquitous throughout the internal part of the Ebro basin, with N-S- and NE-SW-trending faults being predominant in the western (Bardenas Reales) and central (Monegros) sectors of the central part of the Ebro basin, respectively.

Anisotropy of Magnetic Susceptibility: materials and methods

We have sampled 14 sites in Lower and Middle Miocene lacustrine mudrocks; 9 and 5 of these sites at the Bardenas Reales (Fig. 2) and Monegros areas (Fig. 3), respectively. The low-field AMS of 14 or 15 samples per site was measured using an AGICO KLY-2 at the IES "Jaume Almera" (CSIC) in Barcelona (Spain), following the scheme of Jelínek (1977).

The AMS is a second-rank tensor that can be graphically displayed by a three-axis ellipsoid with a given orientation, shape and degree of anisotropy (see Table 1). Analysis of AMS data has been performed following the bootstrap method of Tauxe (1998) (Table 1). The shape and degree of anisotropy of the magnetic ellipsoids has been described using the T and P' parameters of Jelínek (1977), respectively.

Results

Magnetic fabrics

The magnetic susceptibility of the studied mudrocks ranges between 69 and 209×10^{-6} (SI) (Table 1). This indicates that the paramagnetic matrix is probably the major contributor to the bulk susceptibility (Hrouda and Jelínek, 1990). Also, X-ray diffraction results indicate that the magnetic fabric of the studied rocks results from the preferred orientation of phyllosillicate (illite and chlorite) grains.

All the studied sites have P' and T values typical for weakly deformed mudrocks (Table 1). The magnetic fabric of the studied mudrocks can be grouped into three types according to its directional properties. The first type is characterized by a tight clustering of k_{min}

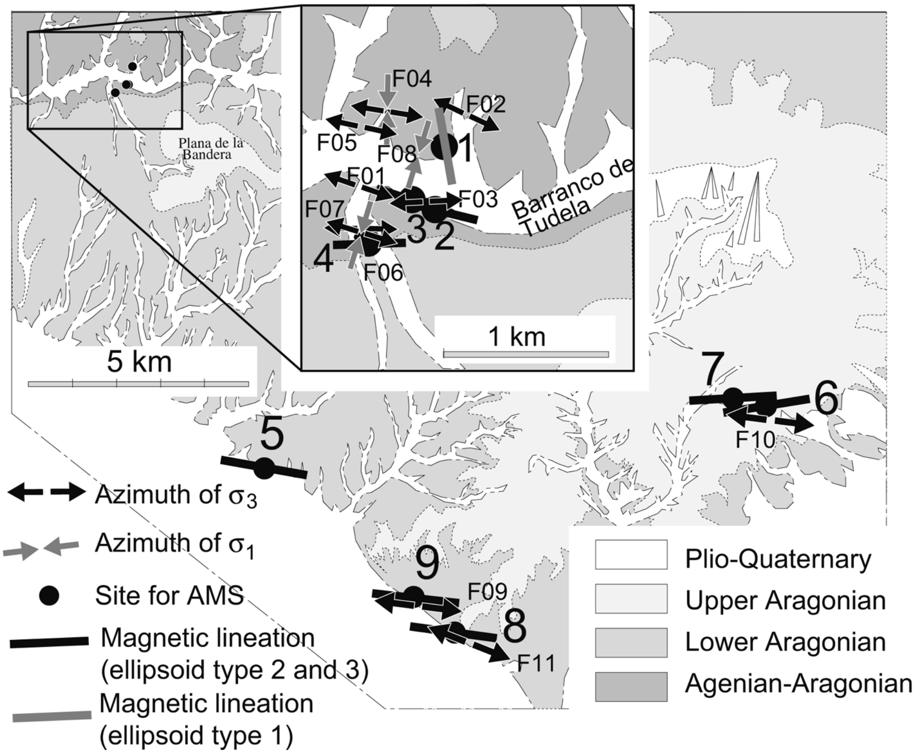

Figure 2. Geological map of the Bardenas Reales area, with location of the studied sites. The inset shows a detailed view of the Barranco de Tudela.

(τ3) around the bedding pole and also by a large dispersion of k_{max} (τ1) and k_{int} (τ2) throughout the bedding plane (e_{12} > 30º). The histograms of bootstrapped eigenvalues indicate that magnetic lineation cannot be statistically distinguished. The second type of magnetic fabric is also characterized by a tight clustering of k_{min} around the bedding pole. k_{max} and k_{int} are also scattered throughout the bedding plane, although their grouping is slightly improved (15º < e_{12} < 30º). The histograms of bootstrapped eigenvalues indicate that, although weak, a magnetic lineation can be distinguished in these sites. In the third type of magnetic fabric, k_{min} remains tightly clustered around the bedding pole, k_{max} and k_{int} appear well grouped (e_{12} < 15º) and a well-defined magnetic lineation appears.

Of all the studied sites, only one from the Bardenas Reales area (Fig. 2) and four from the Monegros area (Fig. 3) have magnetic fabrics of type 1 (i.e. no defined magnetic lineation). The remaining site from the Monegros area (site 10), and all but one site from the Bardenas Reales (site 1), can be included within type 2 (6 sites) and type 3 (3 sites) fabrics (Table 1). In sites with well-defined magnetic lineation, they show a systematic near E-W direction (Figs. 2 and 3).

Discussion

Comparison between AMS and paleostress results

With the exception of site 1, which just shows sedimentary fabric, AMS sites in the Bardenas area (Fig. 2 and Table 1) have their k_{max} axes oriented N098E on average (from the bootstrapped eigenvectors), in striking similitude to the orientation obtained for σ_3 axes (average N101E, according to paleostress solutions from the analyses of strike slip, primary joints and normal faults; Table 2). Locally, the susceptibility axes of some AMS sites are not exactly parallel to the nearest obtained σ_3 axes. Sites 2 and 3 have their k_{max} axes (N103E and N108E, respectively) oblique to the σ_3 axis determined at the closer paleostress site, F03 (N085E, angular difference of 18º and 23º respectively), but they closely parallel the σ_3 axes at the next nearest sites F08 (N112E from a population of 80 strike slip faults) and F01 (N110E, from 47 normal faults), with angular differences below 10º, and a minimum difference of 2º if we just consider sites 3 and F01.

In the Monegros area (Fig. 3 and Table 1), fabrics are not so well developed as in the Bardenas region. Only site 10 shows a well-defined magnetic lineation trending N112E, which also coincides with the orientation of the nearest obtained σ_3 axis (site F12, N116E).

Reliability of magnetic fabric as paleostress indicator

The deformation level both in the Bardenas Reales and Monegros area is weak (i.e. horizon-

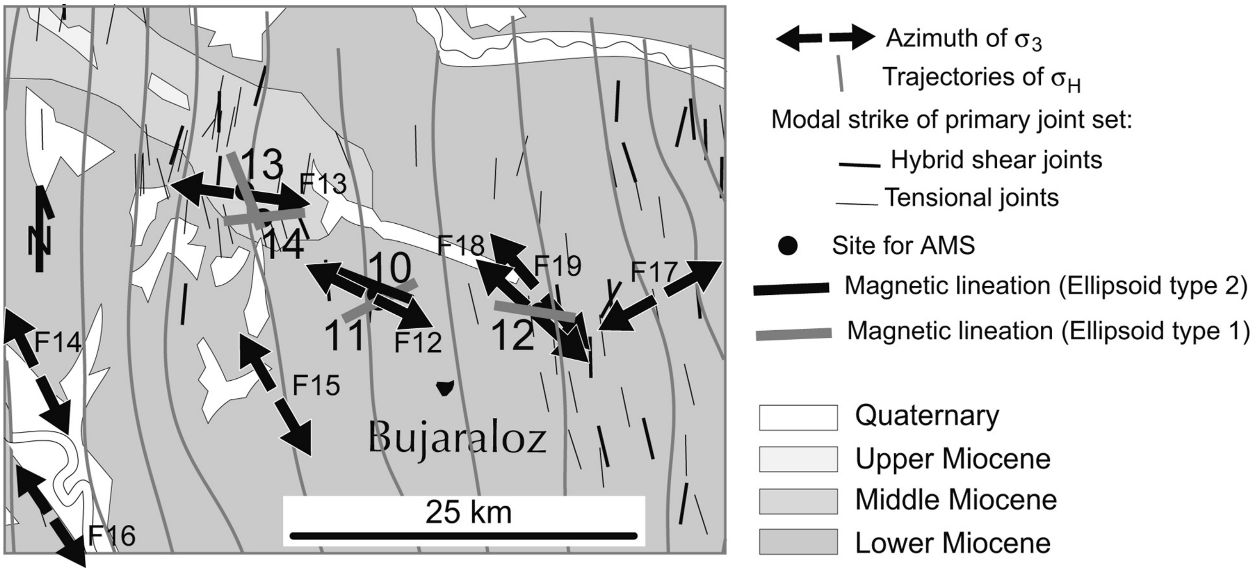

Figure 3. Geological map of the Monegros area, with location of the studied sites.

tal bedding and higher number of joints vs. faults). However, taking into account AMS and paleostress results, the Bardenas Reales area reflects higher deformation conditions, probably related to its nearer position to the south pyrenean front (see Fig. 1). In this area, the magnetic and paleostress ellipsoids are coaxial (Fig. 2). In the Monegros area (Fig. 3), both AMS and paleostress data indicate lower tectonic activity and k_{max} and k_{int} of most sites cannot be statistically distinguished (i.e. magnetic ellipsoid type 1).

SITE	N	K_m	std	P´	std	T	std	t1	D, I (K1)	E1-2 (Jelinek)	E1-2 (Tauxe)
1	14	128.899	10.106	1.018	0.005	0.722	0.110	0.3351	169.1, 3.9	38.2	90.0
2	15	96.469	6.409	1.013	0.002	-0.114	0.186	0.3354	102-6, 3.4	8.9	10.4
3	15	124.185	22.345	1.014	0.002	-0.451	0.211	0.3357	288.3, 0.6	6.7	8.1
4	15	121.541	5.764	1.016	0.003	0.556	0.164	0.3352	268, 4.6	18.3	25.6
5	15	124.931	3.473	1.028	0.003	0.340	0.127	0.3373	100, 2.4	4.6	7.2
6	15	123.734	7.890	1.013	0.002	0.639	0.137	0.3348	261.4, 0.2	10.7	20.6
7	14	98.194	19.590	1.015	0.003	0.641	0.191	0.3350	86.4, 9.1	17.1	29.7
8	15	163.042	20.533	1.017	0.004	0.489	0.300	0.3354	97.8, 9	12.5	22.1
9	14	155.753	18.689	1.021	0.003	0.526	0.267	0.3359	96.6, 5.3	8.1	16.5
10	15	148.385	5.837	1.017	0.003	0.563	0.177	0.3354	111.6, 3.6	9.2	17.8
11	15	188.198	20.060	1.054	0.010	0.789	0.083	0.3390	63, 7.7	14.0	36.2
12	15	115.860	6.866	1.045	0.002	0.810	0.094	0.3379	99.2, 0.1	22.5	41.5
13	15	114.337	9.987	1.031	0.005	0.772	0.109	0.3365	337.8, 2.1	28.0	49.9
14	15	140.293	31.287	1.025	0.006	0.791	0.084	0.3359	83.8, 0.8	24.5	73.5

N = number of specimens
$K_m = (K_{max} + K_{int} + K_{min}) / 3$ (mean susceptibility, in 10^{-6} SI units)
$P' = \exp \{2[(\eta_1 - \eta)^2 + (\eta_2 - \eta)^2 + (\eta_3 - \eta)^2]\}^{1/2}$ (Jelínek, 1981)
$T = [2(\eta_2 - \eta_3) / (\eta_1 - \eta_3)] - 1$ (shape factor; Jelínek, 1981)
std= standard deviation
D, I (K1) = Declination and inclination of K1
E1-2 = semi-angle of the confidence ellipse around K1 from Jelínek's and Tauxe's statistics

Table 1. Summary of magnetic anisotropy results computed for each site.

Site	Explained faults/ total	Kind of tensor	Strike of σ_1	Strike of σ_3	Stress ratio Re
F-01	37/47	Extension	vertical	110	0.42
F-02	6/6	Extension	vertical	099	0.69
F-03	63/80	Extensión	vertical	085	0.23
F-04	11/52	Strike slip	002	092	0.06
	33/52	Extension	vertical	101	0.23
F-05	12/14	Extension	vertical	103	0.10
F-06	28/256	Strike slip	013	102	0.28
	137/256	Extension	vertical	092	0.19
F-07	34/56	Extension	vertical	108	0.48
F-08	62/80	Strike slip	011	112	0.02
F-09	13/15	Extensión	vertical	103	0.28
F-10	16/18	Extension	vertical	101	0.24
F-11	37/52	Extension	vertical	112	0.22
F-12	21/23	Extension	vertical	116	0.02
F-13	8/8	Extension	vertical	097	0.24
F-14	25/28	Extension	vertical	148	0.07
F-15	19/20	Extension	vertical	149	0.07
F-16	18/20	Extension	vertical	146	0.02
F-17	17/18	Extension	vertical	061	0.04
F-18	12/12	Extension	vertical	132	0.00
F-19	13/13	Extension	vertical	139	0.00

Table 2. List of paleostress results obtained at sites with available magnetic anisotropy data.

Conclusions

The coaxiality found between the magnetic and paleostress ellipsoids in the studied area proves the validity of AMS studies as paleostress indicators in foreland basins when sampling is restricted to weakly deformed mudrocks.

Acknowledgements

Financial support was given by two research contracts, Ramón y Cajal Program and JAE-Doc (CSIC) to the Spanish Ministry of Science, to J. C. Larrasoaña and R. Soto, respectively.

References

ALONSO-ZARZA, A. M., ARMENTEROS, A., BRAGA, J. C., MUÑOZ, A., PUJALTE, V., RAMOS, E., AGUIRRE, J., ALONSO-GAVILÁN, G., ARENAS, C., BACETA, J. I., CARBALLEIRA, J., CALVO, J. P., CORROCHANO, A., FORNÓS, J. J., GONZÁLEZ, A., LUZÓN, A., MARTÍN, J. M., PARDO, G., PAYROS, A., PÉREZ, A., POMAR, L., RODRÍGUEZ, J. M. and VILLENA, J. (2002): Tertiary. In: W. GIBBONS and T. MORENO (eds): *The Geology of Spain, Geol. Soc.*: 293-334.

ARLEGUI, L. E. and SIMÓN, J. L. (1998): Reliability of paleostress análisis from fault striations in near multidirectional extension stress field. Example from the Ebro Basin, Spain. *J. Struct. Geol.*, 20: 827-840.

ARLEGUI, L. E. and SIMÓN, J. L. (2001): Geometry and distribution of regional joint sets in non-homogeneous stress field: case study in the Ebro basin (Spain). *J. Struct. Geol.*, 23: 297-313.

BORRADAILE, G. J. and HAMILTON, T. (2004): Magnetic fabrics may proxy as neotectonic stress trajectories, Polis rift, Cyprus. *Tectonics*, 23: *TC1001 1-11*. doi:10.1029/2002TC001434.

HROUDA, F. and JELÍNEK, V. (1990): Resolution of ferromagnetic and paramagnetic anisotropies, using combined low-field and high-field measurements. Geophys. J. Int., 103: 75-84.

JELÍNEK, V. (1977): The statistical theory of measuring anisotropy of magnetic susceptibility of rocks and its applications. In: *Geofyzika*, Brno, 88 pp.

JELÍNEK, V. (1981): Characterization of the magnetic fabrics of rocks. *Tectonophysics*, 79: 63-67.

KISSEL, C., BARRIER, E., LAJ, C. and LEE, T. Q. (1986): Magnetic fabric of "undeformed" marine clays from compressional zones. *Tectonophysics*, 40: 287-308.

MATTEI, M., SAGNOTTI, L., FACCENNA, C. and FUNICIELLO, R. (1997): Magnetic fabric of weakly deformed clayey sediments in the Italian peninsula: relationships with compressional and extensional tectonics. *Tectonophysics*, 271: 107-122.

SIMÓN, J. L., ARLEGUI, L. E., LIESA, C. L. and MAESTRO, A. (1999): Stress perturbations registered by jointing near strike-slip, normal, and reverse faults: examples from the Ebro Basin, Spain. *J. Geophys. Res.*, 104: 15141-15153.

TARLING, D. H. and HROUDA, F. (1993): *The magnetic anisotropy of rocks*. Chapman & Hall, London, 217 pp.

TAUXE, L. (1998): *Paleomagnetic Principles and Practice*. Kluwer Academic Publishers, Dordrecht, 299 pp.